Journal of Organometallic Chemistry 883 (2019) 78–85

Contents lists available at ScienceDirect

Journal of Organometallic Chemistry

journal homepage: www.elsevier.com/locate/jorganchem

Palladium nanoparticles immobilized on the magnetic few layer graphene support as a highly efficient catalyst for ligand free Suzuki cross coupling and homo coupling reactions

Fatemeh Rafiee*, Parvaneh Khavari, Zahra Payami, Narges Ansari

Faculty of Physic-chemistry, Alzahra University, Vanak, Tehran, Iran

ARTICLE INFO

Article history:
Received 3 January 2019
Received in revised form
18 January 2019
Accepted 21 January 2019
Available online 23 January 2019

Keywords:
Graphene
Few layered graphene
Metal–graphene nanocomposite
Palladium nanoparticles
Coupling reaction
Electrochemical exfoliation

ABSTRACT

In this study, we prepared a magnetic metal–graphene nanocomposite for the synthesis of substituted biaryls *via* Suzuki cross coupling and homo coupling reaction of aryl halides. The magnetic few layer graphene composite was synthesized by using one-step electrochemical exfoliation of graphite foil in aqueous iron (II) ammonium sulfate as electrolyte without using of any additive or corrosive media. Then, Fe_2O_3@FLG composite was used an efficient support for the immobilization and suitable dispersing of palladium nanoparticles. The obtained Fe_2O_3@FLG@Pd^0 nanocomposite was characterized using FT-IR, SEM, TEM, EDS, XRD, VSM and ICP-AES analysis. Very low loading of this catalyst was displayed high activity in the producing substituted biaryls. It simply recovered from the reaction mixture and reused without any pre-activation in six consecutive runs with no loss of its catalytic activity or the observation of any detectable palladium leaching process.

1. Introduction

In recent years, graphene has attracted significant attention as one of the most emerging carbon materials due to its excellent properties such as a large specific surface area, electrical conductivity, excellent thermal, chemical, and mechanical stability, and high corrosion resistance [1–7]. Frequently, the exfoliated graphene sheets are in the form of few layer graphene (FLG) and their manufacturing cost is potentially low. Many efforts have been made for the synthesis of large surface area and high quality few layered graphene without agglomerated sheets. In this regard, the electrochemical exfoliation of graphite as emerged as a simple, fast, low-cost, and environmental friendly approach for the few layer graphene production [8–12]. However, the use of acid and ionic liquid electrolyte in the electrochemical exfoliation method causes to damage of the honeycomb lattice of graphene sheets, defects, oxidation processes and functionalization by various groups [13–15]. Therefore, optimized routes under milder conditions without the need for strong oxidizing and corrosive agents are required.

Graphene possesses the ultimate two-dimensional single layer of sp^2-hybridized carbon network that bonded in a hexagonal lattice. Owing to the honeycomb-like structure and 2D morphology, graphene prevents the aggregation of naked nanoparticles, thus it is considered as perfect supports for metal nanoparticles immobilization without surface poisoning problems especially in nanocomposite materials preparation and heterogeneous catalysis applications [16–18]. In addition, the presence of nanoparticles on both sides of the graphene surface inhibits the restacking of graphene sheets and provides higher surface area and better accessibility for reactants [19]. Also, the extended system and high electron density in graphene lead to easier reduction of metal ions and production of catalytically active metal centers [20].

During the past few years, graphene and graphene derivatives represent an attractive alternative to other supports for the immobilization of palladium nanoparticles as catalytic systems for C–C bond formation reactions such as Suzuki cross coupling [21–26] and homo coupling reaction [27]. Palladium nanoparticles enlarging the distance between the graphene sheets and increase the surface area of the composite and thus improve catalytic efficiency [28]. Also, the interaction between graphene and aromatic derivatives in these type reactions may make the reactants easily accessible to the active sites of metal nanoparticles and solead to acceleration in the

* Corresponding author.
E-mail address: f.rafiee@alzahra.ac.ir (F. Rafiee).

https://doi.org/10.1016/j.jorganchem.2019.01.014
0022-328X/

chemical conversion [29,30]. However, the difficulty and time consuming of the catalyst separation methods by common filtration or centrifugation and also dramatically lose catalytic activity in recycling experiments is a limiting factor in the using of graphene heterogeneous catalysts. Along this line, the magnetic separation has developed as a fast separation tool with low cost and high efficiency. The design of graphene based materials decorated with iron oxide nanoparticles and using of magnetic graphene based catalysts in cross coupling reactions has been researched [31–34]. Also, Baaziz and co-workers showed that the introduced iron oxide nanoparticles on the few layer graphene acted as nano-spacers and prevent the restacking of the graphene sheets [19].

Herein, we developed a novel, environmentally-friendly, economic and easy one-step approach to prepare the magnetic few layer graphene as a suitable support for metal nanoparticle immobilization. In continuation of our interest in exploring palladium-catalyzed cross coupling reactions [35–38], in the current work, we immobilized palladium nanoparticles on the surface of Fe_2O_3@FLG support. Then, its catalytic efficiency was investigated in the unsymmetrical biphenyl synthesis *via* ligand free Suzuki cross coupling and also the symmetrical biphenyl synthesis by homo coupling reaction of various aryl halides. The great developments have been performed for the biphenyl synthesis through Suzuki coupling reaction under ligand free conditions such as using of Pd–Pt nanodendrites and Pd–Cu nanowires as highly active catalysts [39,40].

2. Experimental

2.1. Materials and instruments

All chemicals used in this study were commercially available and were purchased from commercial suppliers (Acros, Merck and Aldrich) and used as received without further purification. XRD pattern of the catalyst was recorded with a PW 3710 X-ray diffractometer (Philips) at room temperature using monochromatic Cu Kα radiation with a wavelength of $\lambda = 0.15418$ nm. The peak position and intensity were obtained between 5° and 80° with a rate of 0.04° s^{-1}. Magnetic susceptibility measurements were carried out using a vibrating sample magnetometer (VSM, MDK Co. Ltd, Iran) with the magnetic field range of between +10,000 and −10,000 Oe at room temperature. EDX pattern was recorded using a TESCAN, VEGA 3 LMU instrument. The development of the coupling reactions was monitored using TLC with commercial aluminium-backed plates of silica gel 60 F254 under UV light and an Agilent 6890 GC and GC-MS model Agilent Series 5973. FT-IR spectra were recorded using a Bruker Tensor 27 spectrometer within the 400–4000 cm^{-1} range using KBr disc. ^1H NMR and ^{13}C NMR spectra were recorded with a Brucker avance 400 and 100 MHz machine using $CDCl_3$ as solvent and TMS as standard sample. The morphology of the catalyst was observed using a FE-SEM instrument (HITACHI (S4160) Japan) and TEM (PHILIPS CM30).

2.2. Synthesis of Fe_2O_3@FLG

Graphite foil as an anode and iron as a cathode were used in the electrochemical exfoliation of graphite. Firstly, the surface of electrodes was washed with HCl and methanol. The 0.1 M solution of iron (II) ammonium sulfate (7.8 gr in 200 ml distilled water) was used as the electrolytic solution. The distance between the graphite and Fe electrodes was kept to be ~3 cm throughout the electrochemical process. Electrochemical exfoliation was carried out by applying a positive voltage (10 V) to the graphite electrode for 3 h. After 3 h, the magnetic nanocomposite was separated by a permanent magnet and rinsed several times with distilled water and dried at 100 °C.

2.3. Immobilization of palladium nanoparticles on the surface of Fe_2O_3@FLG

1 g of Fe_2O_3@FLG and 0.02 g (0.12 mmol) of $PdCl_2$ dissolved in 5 ml of HCl and 50 ml H_2O were dispersed using ultrasonic bath for 30 min $NaBH_4$ (0.045 g, 0.12 mmol) was added to the mixture and refluxed for 12 h under stirring. Then, Fe_2O_3@FLG@Pd^0 nanocatalyst was separated by an external magnet and washed several times with ethanol and deionized water and dried in the vacuum oven at 60 °C.

2.4. Typical procedure for the Suzuki-Miyaura cross coupling reaction

Aryl halide (1 mmol), phenylboronic acid (1 mmol), Na_2CO_3 (2 mmol) and Fe_2O_3@FLG@Pd^0 nanocatalyst (0.0004 g) were added to a round-bottomed flask containing 3 mL of aqueous 50% ethanol (v/v%), and the mixture was stirred at 80 °C for the time listed in Table 2. The progress was monitored by TLC ((*n*-hexane or *n*-hexane/EtOAc, 9: 1) or GC. After completion of the reaction, the reaction mixture was cooled to room temperature and the catalyst was separated by an external magnet. Then, the reaction mixture was diluted with water and the resultant mixture extracted with *n*-hexane to isolate the biphenyl products. The combined organic layers were dried over $MgSO_4$, and the solvent was evaporated under reduced pressure.

2.5. Typical procedure for the homo coupling reaction

Aryl halide (1 mmol), K_2CO_3 (1 mmol) and Fe_2O_3@FLG@Pd^0nanocatalyst (0.0001 g) were added to a round-bottomed flask containing 3 mL of DMF. The mixture was stirred at 110 °C for the time specified in Table 4. The mixture was stirred continuously during the reaction and monitored by both TLC (*n*-hexane–EtOAc, 9:1 and 8:2).and GC. When the reaction was complete, the mixture was cooled to room temperature, and the catalyst was separated by an external magnet and then diluted with ether and water. The organic phase was dried over $MgSO_4$, filtered and concentrated under reduced pressure using a rotary evaporator.

3. Result and discussion

3.1. Preparation and characterization of magnetic graphene-base support

To overcome the limitations of electrochemical exfoliation of graphite such as the use of strong acidic media, oxidizing and corrosive reagents, we optimized the conditions and applied iron (II) ammonium sulfate as a mild electrolyte. Often, the synthesis of magnetic graphene based composites required to two-step processes.While, with this method magnetization is performed during electrochemical exfoliation in one step. Then, palladium nanoparticles were immobilized on this surface (Scheme 1).

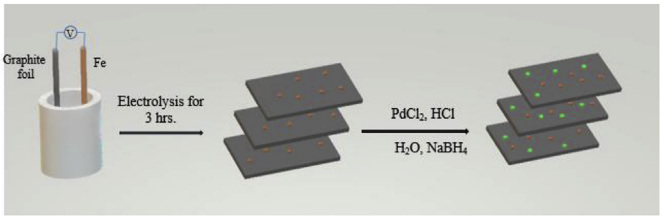

Scheme 1. The preparation of Fe_2O_3@FLG@Pd^0

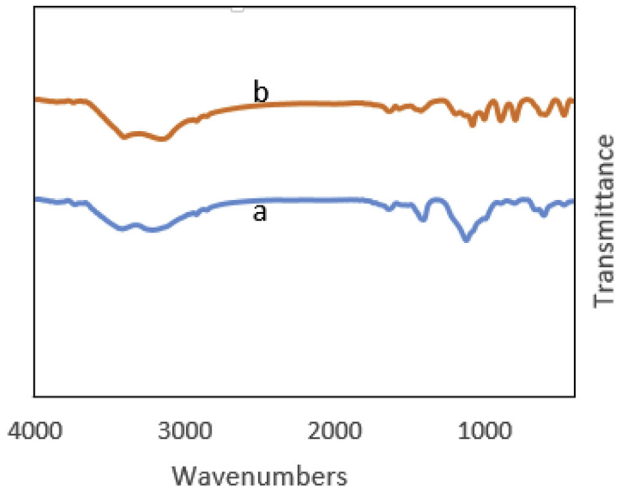

Fig. 1. FT-IR spectra of Fe_2O_3@FLG (a) and Fe_2O_3@FLG@Pd^0nanocomposite (b).

3.2. Characterization of Fe_2O_3@FLG@Pd^0

In the FT-IR spectrum of Fe_2O_3@FLG and Fe_2O_3@FLG@Pd^0 nanocomposite (Fig. 1), the characteristic absorption bands appeared at 3500-3200 (O—H stretching vibration), 2930 and 2855 (C—H stretching vibrations), 1640 and 1512 (C=C stretching vibrations), 1410 and 1100 (CO—H bending vibrations and C—O stretching vibrations, respectively, due to the introducing of a small quantity of oxygen functional groups into FLG surface during the exfoliation process), 1370 and 1340 (C—H bending vibration), 1123 (S=O stretching vibrations, related to the remaining of the electrolyte solution in graphene), and 605 cm^{-1} (Fe—O stretching vibration).

The elemental composition of Fe_2O_3@FLG nanocomposite (a) and Fe_2O_3@FLG@Pd^0 nanocatalyst (b) was determined by energy dispersion spectrometry (EDS) analysis. The EDS spectrums shown in Fig. 2 reveal the presence of Fe (30.37 %W), C (55.36 %W), O (11.75 %W), Cl (0.24 %W) and Pd (2.28 %W) in the prepared catalyst. The exact amount of palladium in the catalyst as determined by

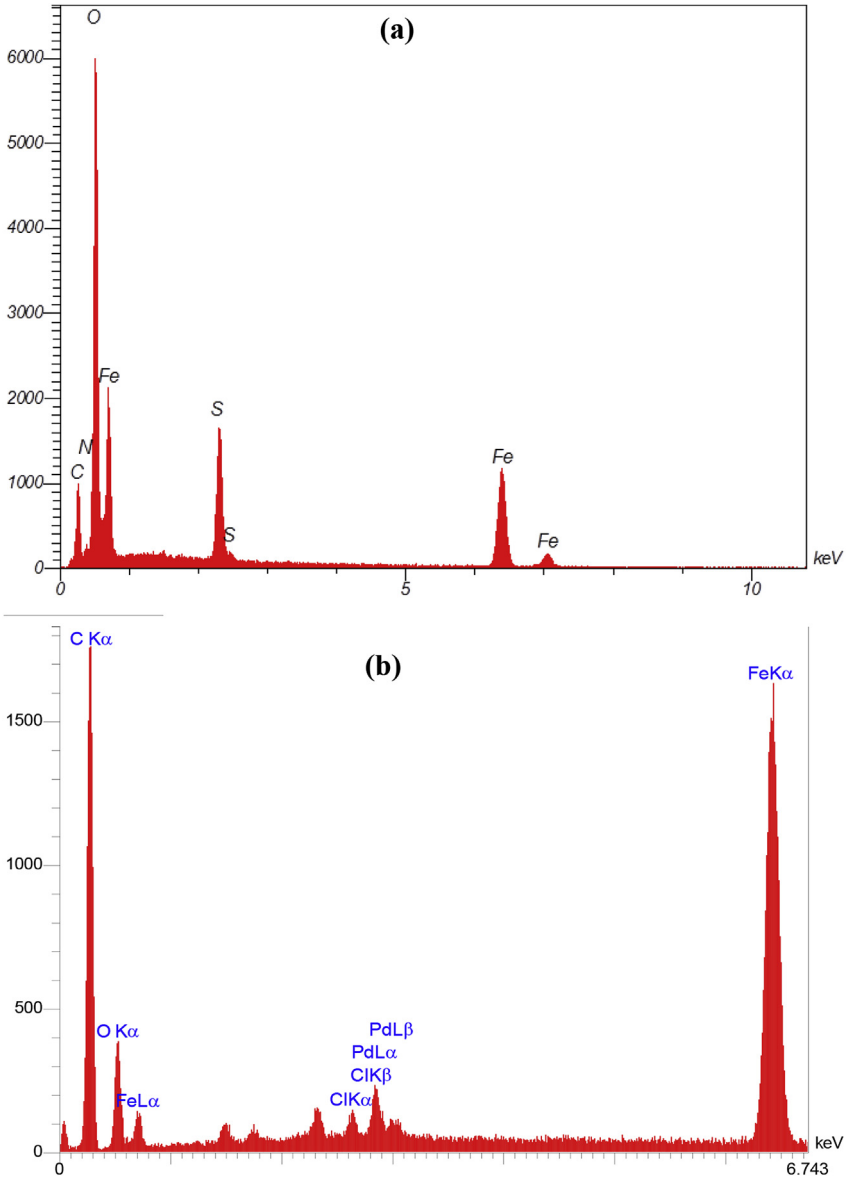

Fig. 2. EDS spectra of Fe_2O_3@FLG (a) and Fe_2O_3@FLG@Pd^0 nanocomposite (b).

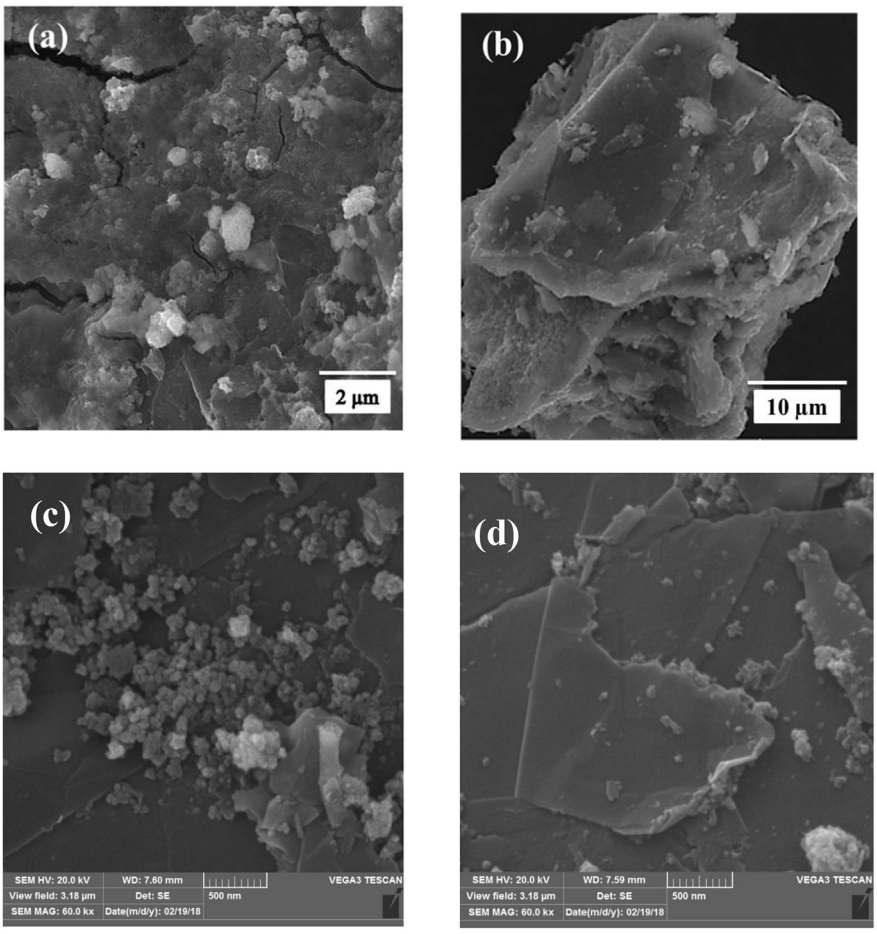

Fig. 3. SEM images of Fe_2O_3@FLG ((a) and (b)) and Fe_2O_3@FLG@Pd^0 nanocomposite ((c) and (d)).

inductively coupled plasma atomic emission spectroscopy (ICP-AES) was 6.42% Wt.(0.6 mmol/g, Pd).

The morphology and size of the nanoparticles were obtained from scanning electron microscopy (SEM) and transmission electron microscopy (TEM) analysis. The FE-SEM photograph (Fig. 3a) of the Fe_2O_3@FLG nanocomposite demonstrates that the graphite is exfoliated and the magnetic nanoparticles are distributed on the surface. Also, the intercalated structure of graphene layers can be observed in Fig. 3b. As seen in the SEM image of nanocatalyst (Fig. 3c and d), iron oxide and palladium nanoparticles well distributed between graphene layers.

The TEM photograph (Fig. 4) shows iron oxide and palladium nanoparticles (dark points) are spherical, narrowly distributed, and well dispersed on the surface of graphene layer (gray layer) with average size less than 10 nm in diameter.

In the powder XRD pattern of the Fe_2O_3@FLG@Pd^0 nanocatalyst (Fig. 5), the diffraction peaks observed at $2\theta = 26.40$, 42.0 and 52.0° correspond, respectively, to the crystalline planes (002), (010), and (004) of few layer graphene.the diffraction peaks at 20.64, 29.43, 35.52, 45.26, 53.41, 57.52 and 62.12° correspond, respectively, to the crystalline planes (111), (220), (311), (400), (422), (511) and (440) of Fe_2O_3, with a cubic spinel structure. The XRD pattern of the nanocatalyst also showed additional peaks at 40.0, 45.32 and 66.93° which are indexed, respectively, to the (111), (200) and (220) crystalline planes of Pd nanocrystals, suggesting the formation of metallic Pd NPs (Pd^0).

The magnetic properties of the Fe_2O_3@FLG@Pd^0nanocatalyst were investigated with a vibrating sample magnetometer at room temperature in an applied magnetic field sweeping from −10 to 10 kOe (Fig. 6). The magnetization curves of the prepared catalyst exhibit no hysteresis loop, indicating superparamagnetic behavior with the saturation magnetization value of 75.46 emu g^{-1}.

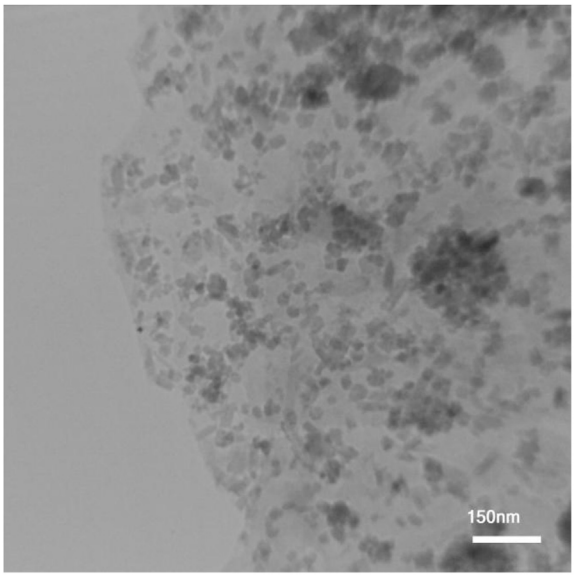

Fig. 4. TEM image of Fe_2O_3@FLG@Pd^0 nanocomposite.

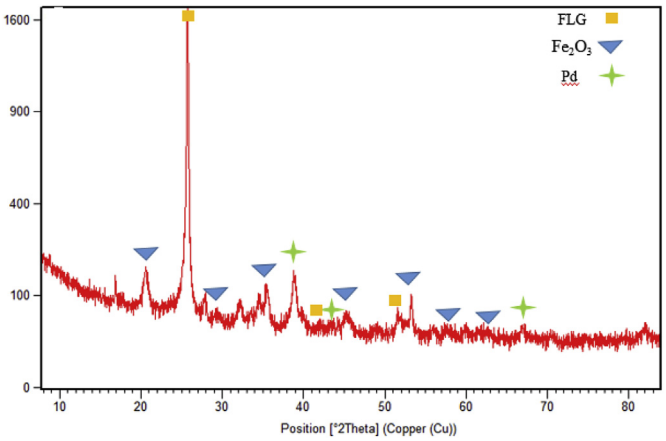

Fig. 5. XRD pattern of the Fe_2O_3@FLG@Pd^0nanocatalyst

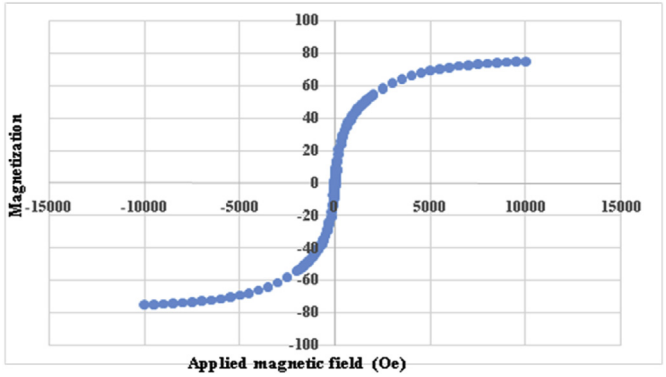

Fig. 6. Room temperature magnetization curve of Fe_2O_3@FLG@Pd^0

3.3. Catalytic activity examinations in Suzuki cross coupling

In continuation of our recent investigations on the synthesis and applications of the heterogeneous magnetic palladium complex in coupling reactions, we now report the preparation of a magnetic graphene base nanocatalyst. At the first, the catalytic activity of the Fe_2O_3@FLG@Pd^0 catalyst was examined in the Suzuki cross-coupling reaction. In an effort to develop an optimized catalytic system, the reaction of 1-bromo-4-chloro-benzene and phenylboronic acid was selected as the model reaction and the effects of solvent, base and amount of catalyst were examined.

As it can be seen from Table 1, the best performance on outcome of reaction was observed using aqueous ethanol (EtOH: H_2O (1:1)) as solvent and Na_2CO_3 as the best base. This cross coupling reaction was conducted at different temperatures. The reaction time was reduced with increasing of temperature. Also, we was studied the effect of catalyst loading on the conversion. No desirable product was obtained in the absence of catalyst, (Table 1, entry 12), indicating the essential of use of the catalyst for reaction progressing. Use of lower amounts of catalyst led to relatively longer reaction times. The best results were obtained with 0.0004 g of nanocatalyst (mol% Pd).

To explore the efficiency and the scope of the procedure, the optimized conditions were extended to a variety of substituted aryl halides and phenylboronic acids (Scheme 2).

As is evident from the results (Table 2), this catalytic system is compatible with a wide range of functional groups. The presence of either electron-releasing (Me, OMe and NH_2 on the aryl halides and Me and OMe on the phenylboronic acids) or electron withdrawing substituents (CN, CHO, COMe and Cl on the aryl halides and F on the phenylboronic acid) has no significant sensitivity in the product yields and reaction times. Also thiophen-2-ylboronic acid was applied as a heteroarylboronic acid (Table 2, entries 18 and 19). The cross coupling reaction of 1-bromo-4-chloro-benzene with various phenylboronic acids was carried out (Table 2, entries 4, 15 and 19) to study the process chemoselectivity. In these reactions only Br was substituted due to the less reactivity of Cl as leaving group.

3.4. The recovery and reusability of the catalyst

The reusability and recyclability experiments were performed for this catalyst through coupling reaction of 1-bromo-4-chloro-benzene with phenylboronic acid as a model reaction under optimized conditions. After completion of the first cycle, the catalyst was recovered magnetically from the reaction mixture and washed with ethanol to remove the residual product. The recovered catalyst was dried and then directly carried forward to the next run with fresh reactants and solvent under the same conditions. As shown in Fig. 7, the catalyst can be reused up to six runs without observing any loss of activity.

The hot filtration test was also carried out to investigate the lack of the homogeneous palladium species which is formed *via*

Table 1
Optimization of reaction conditions for the Suzuki cross coupling reaction.[a].

Entry	Solvent	Base	Catalyst (g)	Temp. (°C)	Time (min)	Conversion (%)
1	H_2O	K_2CO_3	0.0005	rt	180	–
2	H_2O	K_2CO_3	0.0005	reflux	180	–
3	EtOH	K_2CO_3	0.0005	rt	60	90
4	EtOH	K_2CO_3	0.0005	reflux	30	100
5	EtOH/H_2O (1:1)	K_2CO_3	0.0005	rt	120	–
6	EtOH/H_2O (1:1)	K_2CO_3	0.0005	reflux	15	100
7	EtOH/H_2O (1:1)	K_2CO_3	0.0003	80	35	100
8	EtOH/H_2O (1:1)	Na_2CO_3	0.0003	80	20	100
9	EtOH/H_2O (1:1)	NaOAc	0.0003	80	30	100
10	EtOH/H_2O (1:1)	$NaHCO_3$	0.0003	80	45	100
11	EtOH/H_2O (1:1)	$KHCO_3$	0.0003	80	35	100
12	EtOH/H_2O (1:1)	Na_2CO_3	–	80	180	–
13	EtOH/H_2O (1:1)	Na_2CO_3	0.0002	80	30	100
14	EtOH/H_2O (1:1)	Na_2CO_3	0.0004	80	5	100
15	EtOH/H_2O (1:1)	Na_2CO_3	0.0004	60	15	100

[b]GC (*n*-hexane as internals standard) and TLC (*n*-hexane or *n*-hexane: ethyl acetate 9:1) conversions.
[a] Reactions conditions: *p*-Cl–Ph–Br (1 mmol), $PhB(OH)_2$ (1 mmol), base (2 mmol), nanocatalyst (g), solvent (3.0 ml).

Table 2
Suzuki cross-coupling reaction of various aryl halides.[a].

Entry	Ar-X	$ArB(OH)_2$	Time (min)	Yield[b] (%)[b]	TON[c]	TOF[d]
1	Ph–Br	$PhB(OH)_2$	15	98	4083	16332
2	*p*-OHC–PhBr	$PhB(OH)_2$	20	97	4041	12123
3	*p*-Me–Ph–I	$PhB(OH)_2$	10	100	4167	25002
4	*p*-Cl–Ph–Br	$PhB(OH)_2$	5	99	4125	49500
5	*p*-NC–Ph–Br	$PhB(OH)_2$	10	96	4000	24000
6	*p*-MeOC–Ph–Br	3,4,5-tri-flouro-$PhB(OH)_2$	15	97	4041	16164
7	*p*-Br-Ph–Br	3,4,5-tri-flouro-$PhB(OH)_2$	10	95	3958	23748
8	*p*-MeO–Ph–I	3,4,5-tri-flouro-$PhB(OH)_2$	15	100	4167	27780
9	*p*-NC–Ph–Cl	*p*-Me–$PhB(OH)_2$	120	94	3917	1958
10	*p*-Me–Ph–I	*p*-Me–$PhB(OH)_2$	10	100	4167	25002
11	*p*-MeO–Ph–I	*p*-Me–$PhB(OH)_2$	15	98	4083	16332
12	Ph–Br	*p*-Me–$PhB(OH)_2$	10	99	4125	24750
13	*p*-H_2N–Ph–Br	*m*-MeO–$PhB(OH)_2$	20	94	3917	11751
14	*p*-OHC–Ph–Br	*m*-MeO–$PhB(OH)_2$	15	96	4000	16000
15	*p*-Cl–Ph–Br	*m*-MeO–$PhB(OH)_2$	10	97	4041	24246
16[e]	*p*-Br-Ph–Br	*m*-MeO–$PhB(OH)_2$	15	95	3958	15832
17	Ph–Cl	*m*-MeO–$PhB(OH)_2$	180	45	1875	625
18	*p*-Me–Ph–I	Thiophene-$B(OH)_2$	30	92	3833	7666
19	*p*-Cl–Ph–Br	Thiophene-$B(OH)_2$	30	70	2917	5834

[a] Reaction conditions: aryl halide (1 mmol), phenylboronic acid (1 mmol), Na_2CO_3 (2 mmol), nanocatalyst (0.0004 g, mol% Pd), H_2O: EtOH (1:1) (3 ml), 80 °C.
[b] Isolated yield. Full conversions (100%) were achieved in all cases except entries 17 and 19.
[c] Turnover number: moles of product per mole of Pd.
[d] Turnover frequency: moles of product per mole of Pd per hour.
[e] ArX:$ArB(OH)_2$ (1:2).

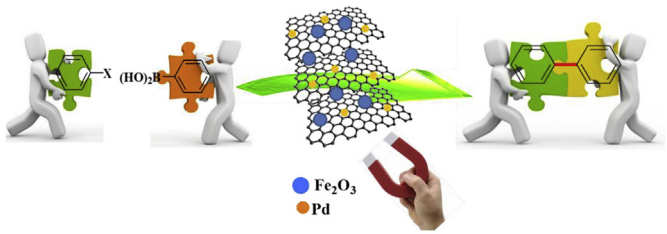

Scheme 2. Suzuki cross coupling reaction by Fe_2O_3@FLG@Pd^0 catalyst.

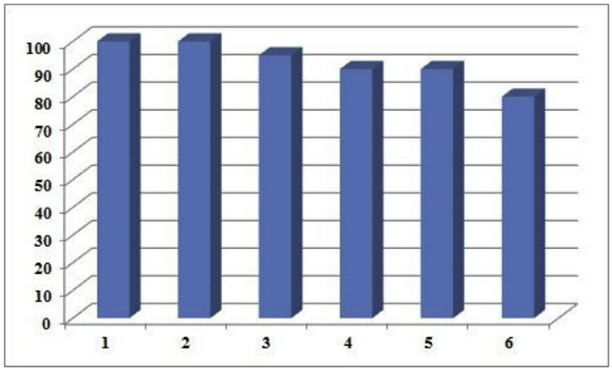

Fig. 7. Reusability of the Fe_2O_3@FLG@Pd^0 catalyst.

leaching during the cross coupling reaction. In a typical reaction, a mixture of 0.0004 g of the Fe_2O_3@FLG@Pd^0 catalyst in 3 mL water: ethanol (1:1) was prepared and left to stir at 80 °C for 10 min, and then the catalyst was magnetically removed from the hot reaction mixture. 1-Bromo-4-chlorobenzene, phenylboronic acid and Na_2CO_3 were added to the filtrate and continued at 80 °C for the time specified in Table 2. The filtrate showed no catalytic activity and no coupling product was detected, indicating that no catalytically active palladium remained in the filtrate.

To show the merit of the present work, we compared the achieved results with the previously reported graphene-based palladium catalysts in the synthesis of 4-methyl-biphenyl *via* cross coupling of 1-iodo-4-methyl-benzene with phenylboronic acid (Table 3). The results obtained with this catalytic system are superior to others in terms of catalytic efficiency (higher TON and TOF), so that it gave a better yield in shorter time with lower loading of palladium catalyst under mild reaction conditions.

3.5. Catalytic activity studies in homo coupling reaction

In continuation of the investigation of catalyst efficiency, we also evaluated the catalytic activity of Fe_2O_3@FLG@Pd^0 catalyst in the homo coupling reaction of aryl halides. To find the best experimental conditions, the homo coupling reaction of 1-bromo-4-chloro-benzene was carried out with K_2CO_3 as base and using different solvents. As presented in Table 4, the best results were obtained in DMF at 110 °C and 0.0001 g of nanocatalyst (mol% Pd).

With the optimum reaction conditions in hand, this catalytic system was applied for the homo coupling reaction of various aryl halides (Scheme 3). Electron-withdrawing (NO_2, CN, COMe, Cl and Br) and electron-donating (Me, OMe and NH_2) aryl halides produced symmetrical biphenyl products efficiently (Table 5).

4. Conclusions

In conclusion, a nano-sized magnetic graphene nanocomposite with high magnetic and excellent dispersibility was prepared by electrochemical exfoliation of graphite foil. One-step synthesis, environmentally-friendly route, mild conditions (acid and corrosive material free) and simple reaction set up are the advantages of proposed methodology. After the immobilization of palladium nanoparticles, the efficiency of prepared catalyst was investigated in coupling reactions. Symmetrical and unsymmetrical biphenyls were obtained in high yields at short reaction times.

Table 3
Comparison of catalytic performance of Fe_2O_3@FLG@Pd^0 with different graphene-based palladium catalysts in the coupling reaction of 1-iodo-4-methyl-benzene and phenylbronic acid.

Entry	Catalytic system	Conditions	Time	Yield (%)	TON	TOF	Ref.
1	GA@FSNP@Pd (0.28 mol %)	Solvent-free 90 °C	0.5	88	314	628	[41]
2	Pd–Fe_3O_4/rGO (0.06 mol %)	H_2O:EtOH (1:1) 80 °C	0.5	96	1600	3200	[31]
3	GO/NHC–Pd (1 mol %)	H_2O 100 °C	12 h	70.5	70.5	5.87	[21]
4	GO-CPTMS@Pd-TKHPP (10 mol %)	H_2O:EtOH (1:2) 80 °C	10 min	97	9.7	58.2	[22]
5	GO/Fe_3O_4/PAMPS/Pd (0.2 mol %)	H_2O:EtOH (1:1) 80 °C	2	100	500	250	[34]
6	GO–NHC–Pd (1 mol %),	DMF:H_2O (1:1) 50 °C	1	94	94	94	[42]
7	NHC–Pd/GO-IL (0.1 mol %)	H_2O:EtOH (1:1) 60 °C	2.5	98	980	392	[43]
8	Pd/Nf–G (0.3 mol %)	H_2O:EtOH (1:1) 80 °C	1.5	93	310	206.7	[26]
9	Pd–Ni(20)/RGO (0.018 mol% Pd)	H_2O:EtOH (1:1) 30 °C	9	96.4	5355.5	595.1	[44]
10	GO–2N–Pd(II) (0.5 mol %)	EtOH 80 °C	0.5	99	198	396	[45]
11	Pd NPs-HNG (0.025 mol)	H_2O:EtOH (1:1) 60 °C	2.5	98	3920	1568	[24]
12	Fe_2O_3@FLG@Pd^0 0.024	H_2O:EtOH (1:1) 80 °C	10 min	100	4167	25002	This work

Table 4
Optimization of reaction conditions for the homo coupling reaction.[a].

Entry	Solvent	Catalyst (g)	Temp. (°C)	Time (min)	Conversion (%)
1	H_2O	0.0004	80	180	–
2	$PhCH_3$	0.0004	100	180	–
3	EtOH	0.0004	70	180	20
4	CH_3CN	0.0004	80	180	–
5	DMF	0.0004	110	120	100
6	DMF	0.0002	110	80	100
7	DMF	0.0001	110	40	100
8	DMF	–	110	180	–

[b]GC (*n*-hexane as internals standard) and TLC (*n*-hexane or *n*-hexane: ethyl acetate 9:1) conversions.
[a] Reactions conditions: *p*-Cl–Ph–Br (1 mmol), $PhB(OH)_2$ (1 mmol), K_2CO_3 (1 mmol), nanocatalyst (g), solvent (3.0 ml).

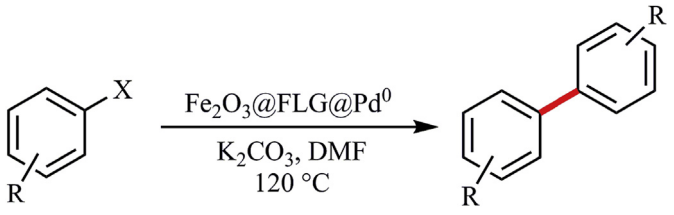

Scheme 3. Homo coupling reaction of aryl halides by Fe_2O_3@FLG@Pd^0 catalyst.

Table 5
Homo-coupling reaction of various aryl halides.[a].

Entry	Ar-X	Ar– Ar	Time (min)	Yeild (%)[b]
1	*m*-O_2N–Ph–I	*m*-O_2N–Ph–Ph–*m*-NO_2	40	94
2	*p*-Me–Ph–I	*p*-Me–Ph–Ph–*p*-Me	25	97
3	*p*-MeO–Ph–I	*p*-MeO–Ph–Ph–*p*-OMe	30	95
4	Ph–Br	Ph–Ph	40	98
5	*p*-NC–Ph–Br	*p*-NC–Ph––Ph–*p*-CN	45	94
6	*p*-Br–Ph–Br	*p*-Br–Ph–Ph–*p*-Br	50	93
7	*p*-Cl–Ph–Br	*p*-Cl–Ph–Ph–*p*-Cl	40	96
8	*p*-MeOC–Ph–Br	*p*-MeOC–Ph–Ph–*p*-COMe	50	92
9	*p*-H_2N–Ph–Br	*p*-H_2N–Ph––Ph–NH_2	45	90

[a] Reaction conditions: aryl halide (1 mmol), K_2CO_3 (1 mmol), nanocatalyst (0.0001 g), DMF (3 ml), 110 °C.

Acknowledgements

We gratefully acknowledge the partial financial support received from the research council of Alzahra University.

References

[1] V.B. Mohan, K. Lau, D. Hui, D. Bhattacharyya, Graphene-based materials and their composites: a review on production, applications and product limitations, Compos. B Eng. 142 (2018) 200–220.
[2] V. Singh, D. Joung, L. Zhai, S. Das, S.I. Khondaker, S. Seal, Graphene based materials: past, present and future, Prog. Mater. Sci. 56 (2018) 1178–1271.
[3] Y. Zhong, Z. Zhen, H. Zhu, Graphene: fundamental research and potential applications, FlatChem 4 (2017) 20–32.
[4] C.N.R. Rao, A.K. Sood, Graphene Synthesis, Properties, and Phenomena, Wiley-VCH, Weinheim, 2013.
[5] B.F. Machado, P. Serp, Graphene-based materials for catalysis, Catal. Sci. Technol. 2 (2012) 54–75.
[6] X. Huang, X. Qi, F. Boey, H. Zhang, Graphene-based composites, Chem. Soc. Rev. 41 (2012) 666–686.
[7] V. Georgakilas, M. Otyepka, A.B. Bourlinos, V. Chandra, N. Kim, K.C. Kemp, P. Hobza, R. Zboril, K.S. Kim, Functionalization of graphene: covalent and non-covalent approaches, derivatives and applications, Chem. Rev. 112 (2012) 6156–6214.
[8] L. Li, M. Wang, M. Cao, H. Qiu, Z. Yang, L. Xu, J. Li, Regulation of radicals from electrochemical exfoliation for production of graphene and its electrochemical properties, Electrochim. Acta 258 (2017) 1484–1492.
[9] H. Wang, C. Wei, K. Zhu, Y. Zhang, C. Gong, J. Guo, J. Zhang, L. Yu, J. Zhang, Preparation of graphene sheets by electrochemical exfoliation of graphite in confined space and their application in transparent conductive films, ACS Appl. Mater. Interfaces 9 (2017) 34456–34466.
[10] X. Huang, S. Li, Z. Qi, W. Zhang, W. Ye, Y. Fang, Low defect concentration few-layer graphene using a two-step electrochemical exfoliation, Nanotechnology 26 (2015) 105602–105607.
[11] N. Parveen, M.O. Ansari, M.H. Cho, Simple route for gram synthesis of less defective few layered graphene and its electrochemical performance, RSC Adv. 5 (2015) 44920–44927.
[12] J. Liu, M. Notarianni, G. Will, V.T. Tiong, H. Wang, N. Motta, Electrochemically exfoliated graphene for electrode films: effect of graphene flake thickness on the sheet resistance and capacitive properties, Langmuir 29 (2013) 13307–13314.
[13] C.Y. Su, A.Y. Lu, Y. Xu, F.R. Chen, A.N. Khlobystov, L.J. Li, High-quality thin graphene films from fast electrochemical exfoliation, ACS Nano 5 (2011) 2332–2339.
[14] N. Liu, F. Luo, H. Wu, Y. Liu, C. Zhang, J. Chen, One-step ionic-liquid-assisted electrochemical synthesis of ionic-liquid-functionalized graphene sheets directly from graphite, Adv. Funct. Mater. 18 (2008) 1518–1525.
[15] N.G. Shang, P. Papakonstantinou, S. Sharma, G. Lubarsky, M. Li, D.W.M. Neill,

A.J. Quinn, W. Zhoue, R. Blackley, Controllable selective exfoliation of high-quality graphene nanosheets and nanodots by ionic liquid assisted grinding, Chem. Commun. 48 (2012) 1877–1879.
[16] P.B. Rathod, Graphene/nanoparticles composites synthesis and application, Int. J. Appl. Res. 1 (2015) 752–758.
[17] M. Khan, M.N. Tahir, S.F. Adil, H.U. Khan, M.R.H. Siddiqui, A.A. Al-warthan, W. Tremel, Graphene based metal and metal oxide nanocomposites: synthesis, properties and their applications, J. Mater. Chem. A. 3 (2015) 18753–18808.
[18] M. Kwak, S. Lee, D. Kim, S.K. Park, Y. Piao, Facile synthesis of Au-graphene nanocomposite for the selective determination of dopamine, J. Electroanal. Chem. 776 (2016) 66–73.
[19] W. Baaziz, L. Truong-Phuoc, C. Duong-Viet, G. Melinte, I. Janowska, V. Papaefthimiou, O. Ersen, S. Zafeiratos, D. Begin, S. Begin-Colin, C. Pham-Huu, Few layer graphene decorated with homogeneous magnetic Fe_3O_4 nanoparticles with tunable covering densities, J. Mater. Chem. 2 (2014) 2690–2700.
[20] H.A. Elazab, A.R. Siamaki, S. Moussa, B.F. Gupton, M.S. El-Shall, Highly efficient and magnetically recyclable graphene-supported Pd/Fe_3O_4 nanoparticle catalysts for Suzuki and Heck cross-coupling reactions, Appl. Catal., A 491 (2015) 58–69.
[21] S. Kim, H.J. Cho, D.S. Shin, S.M. Lee, Recyclable and eco-friendly Pd-complexed graphene oxide/Nheterocyclic carbene catalyst for various coupling reactions in aqueous phase, Tetrahedron Lett. 58 (2017) 2421–2425.
[22] K. Bahrami, S. Nakhjiri Kamrani, Synthesis, characterization and application of graphene palladium porphyrin as a nanocatalyst for the coupling reactions such as: Suzuki-Miyaura and Mizoroki-Heck, Appl. Organomet. Chem. 32 (2018) e4102.
[23] S. Rana S. Maddila, K. Yalagala, S.B. Jonnalagadda, Organo functionalized graphene with Pd nanoparticles and its excellent catalytic activity for Suzuki coupling reaction, Appl. Catal., A 505 (2015) 539–547.
[24] S. Kazemi Movahed, M. Dabiri, A. Bazgir, Palladium nanoparticles decorated high nitrogen doped graphene with high catalytic activity for Suzuki-Miyaura and Ullmann-type coupling reactions in aqueous media, Appl. Catal., A 488 (2014) 265–274.
[25] M. Sarvestani, R. Azadi, Palladium nanoparticles deposited on a graphene–benzimidazole support as an efficient and recyclable catalyst for aqueous-phase Suzuki–Miyaura coupling reaction, Appl. Organomet. Chem. 31 (2017), e3667.
[26] S.S. Shendage, U.B. Patil, J.M. Nagarkar, Electrochemical synthesis and characterization of palladium nanoparticles on nafion–graphene support and its application for Suzuki coupling reaction, Tetrahedron Lett. 54 (2013) 3457–3461.
[27] Z.J. Wang, J.J. Lv, R.N. Yi, M. Xiao, J.J. Feng, Z.W. Liang, A.J. Wang, X. Xu, Nondirecting group sp^3 C–H activation for synthesis of bibenzyls *via* homo-coupling as catalyzed by reduced graphene oxide supported PtPd@Pt porous nanospheres, Adv. Synth. Catal. 360 (2018) 932–941.
[28] M. Gómez-Martínez, E. Buxaderas, I.M. Pastor, D.A. Alonso, Palladium nanoparticles supported on graphene and reduced graphene oxide as efficient recyclable catalyst for the Suzuki–Miyaura reaction of potassium aryltrifluoroborates, J. Mol. Catal. Chem. 404 (2015) 1–7.
[29] J.F. Hu, Y. Wang, M. Han, Y. Zhou, X. Jiang, P.P. Sun, A facile preparation of palladium nanoparticles supported on magnetite/s-graphene and their catalytic application in Suzuki–Miyaura reaction, Catal. Sci. Technol. 2 (2012) 2332–2340.
[30] G.M. Scheuermann, L. Rumi, P. Steurer, W. Bannwarth, R. Mulhaupt, Palladium nanoparticles on graphite oxide and its functionalized graphene derivatives as highly active catalysts for the Suzuki–Miyaura coupling reaction, J. Am. Chem. Soc. 131 (2009) 8262–8270.
[31] W. Fu, Z. Zhang, P. Zhuang, J. Shen, M. Ye, One-pot hydrothermal synthesis of magnetically recoverable palladium/reduced graphene oxide nanocomposites and its catalytic applications in cross-coupling reactions, J. Colloid Interface Sci. 497 (2017) 83–92.
[32] S.J. Hoseini, V. Heidari, H. Nasrabadi, Magnetic Pd/Fe_3O_4/reduced-graphene oxide nanohybrid as an efficient and recoverable catalyst for Suzuki-Miyaura coupling reaction in water, J. Mol. Catal. Chem. 396 (2015) 90–95.
[33] X. Zhao, X. Liu, A novel magnetic $NiFe_2O_4$@graphene–Pd multifunctional nanocomposite for practical catalytic application, RSC Adv. 5 (2015) 79548–79555.
[34] S. Asadi, R. Sedghi, M.M. Heravi, Pd Nanoparticles immobilized on supported magnetic GO@PAMPS as an auspicious catalyst for Suzuki–Miyaura coupling reaction, Catal. Lett. 147 (2017) 2045–2056.
[35] F. Rafiee, Synthesis of phenanthridine and phenanthridinone derivatives based on Pd-catalyzed C–H activation, Appl. Organomet. Chem. 31 (2017) e3820.
[36] F. Rafiee, N. Mehdizadeh, Palladium N-heterocyclic carbene complex of vitamin B1 supported on silica-coated Fe_3O_4 nanoparticles: a green and efficient catalyst for C–C coupling, Catal. Lett. 148 (2018) 1345–1354.
[37] F. Rafiee, N. Mehdizadeh, A green synthesis of biaryls in water catalyzed by palladium nanoparticles immobilized on *N*-amidinoglycine-functionalized iron oxide nanoparticles, Transition Met. Chem. 43 (2018) 295–300.
[38] F. Rafiee, S.A. Hosseini, CNC pincer palladium complex supported on magnetic chitosan as highly efficient and recyclable nanocatalyst in C–C coupling reactions, Appl. Organomet. Chem. 32 (2018), e4519.
[39] Z.J. Wang, J.J. Lv, J.J. Feng, N. Li, X. Xu, A.J. Wang, R. Qiu, Enhanced catalytic performance of Pd–Pt nanodendrites for ligand-free Suzuki cross-coupling reactions, RSC Adv. 5 (2015) 28467–28473.
[40] J.J. Lv, Z.J. Wang, J.J. Feng, R. Qiu, A.J. Wang, X. Xu, Facile synthesis of highly active Pd-Cu nanowires catalyst through a simple wet-chemical strategy for ligand-free Suzuki cross coupling reaction, Appl. Catal., A 522 (2016) 188–193.
[41] M. Tanhaei, A. Mahjoub, R. Nejat, Three-Dimensional Graphene–Magnetic Palladium Nanohybrid: a highly efficient and reusable catalyst for promoting organic reactions, Catal. Lett. 148 (2018) 1549–1561.
[42] J.H. Park, F. Raza, S.J. Jeon, H.I. Kim, T.W. Kang, D. Yim, J.H. Kim, Recyclable N-heterocyclic carbene/palladium catalyst on graphene oxide for the aqueous-phase Suzuki reaction, Tetrahedron Lett. 55 (2014) 3426–3430.
[43] S.K. Movahed, R. Esmatpoursalmani, A. Bazgir, *N*-Heterocyclic carbene palladium complex supported on ionic liquid-modified graphene oxide as an efficient and recyclable catalyst for Suzuki reaction, RSC Adv. 4 (2014) 14586–14591.
[44] R. Nie, J. Shi, W. Du, Z. Hou, Ni_2O_3-around-Pd hybrid on graphene oxide: an efficient catalyst for ligand-free Suzuki–Miyaura coupling reaction, Appl. Catal. Gen. 473 (2014) 1–6.
[45] C. Bai, Q. Zhao, Y. Li, G. Zhang, F. Zhang, X. Fan, Palladium complex immobilized on graphene oxide as an efficient and recyclable catalyst for Suzuki coupling reaction, Catal. Lett. 144 (2014) 1617–1623.